

Structural properties of nickel manganite $\text{Ni}_x\text{Mn}_{3-x}\text{O}_4$ with $0.5 \leq x \leq 1$

R. LEGROS, R. METZ, A. ROUSSET

Laboratoire de Chimie des Matériaux Inorganiques, C.N.R.S. URA 1311,
Université Paul Sabatier, 118 Route de Narbonne, 31062 Toulouse Cedex, France

Single-phase nickel manganite spinels, $\text{Ni}_x\text{Mn}_{3-x}\text{O}_4$, with $0.5 \leq x \leq 1$, were prepared by a careful thermal processing of nickel-manganese coprecipitated oxalate precursors. Powder X-ray diffraction analysis of the spinel revealed the presence of cubic single spinel phase with parameter a which decreases with nickel content. The lattice parameter variation can be explained in terms of the distribution of Ni^{2+} ions on the octahedral sites. Therefore, a fine analysis of data shows that some Ni^{2+} ions (for $x > 0.56$) are located in tetrahedral sites. The percentage of nickel in A-sites increases with nickel content (x) following the relation

$$\% \text{Ni}^{2+} \text{ in A sites} = P = -82.1x^2 + 192.4x - 81.5$$

and thus the general formula for cation distribution is



This relationship explains the electrical properties of semiconducting nickel manganite ceramics.

1. Introduction

Interest in transition metal manganite $\text{Mn}_{3-x}\text{M}_x\text{O}_4$ ($0 \leq x \leq 1$ and $M = \text{nickel, cobalt, etc.}$) for use in thermally sensitive resistors (negative temperature coefficient thermistors) has been shown in several previous papers [1-5]. In these compounds the electrical conductivity is due to the transfer of electrons (hopping) between the Mn^{3+} and Mn^{4+} ions in an octahedral sublattice of the spinel structure [6]. Thus the electrical properties are strongly related to the cation concentration and distribution among the two sublattices. In connection with this, an important controversy exists even for a relatively simple phase such as nickel manganite, NiMn_2O_4 , despite of a number of investigations [7-16] the results of which are summarized in Table I.

By regulating the amount of nickel in nickel manganite, $\text{Mn}_{3-x}\text{Ni}_x\text{O}_4$, we have shown previously [2] that it is possible to vary the resistivity between 100 000 and 1500 Ωcm . Thus this material plays an important role in industrial applications.

In this paper, a cation distribution in the defined compound, Mn_2NiO_4 , is proposed, taking into account the results obtained for a complete range of solid solutions $\text{Mn}_{3-x}\text{Ni}_x\text{O}_4$ with $0.5 \leq x \leq 1$. This method seems to be more relevant than considering only the defined compound Mn_2NiO_4 .

2. Experimental procedure

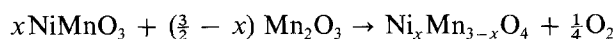
2.1. Preparation of nickel manganite powders

The powders result from the decomposition of oxalic precursors $\text{Mn}_{1-y}\text{Ni}_y(\text{C}_2\text{O}_4) \cdot 2\text{H}_2\text{O}$. Taking into

account the isomorphism of manganese and nickel oxalate, the latter compound was prepared by coprecipitation in aqueous solution from $\text{MCl}_2 \cdot 6\text{H}_2\text{O}$ ($M = \text{manganese, nickel}$) and ammonium oxalate $(\text{NH}_4)_2\text{C}_2\text{O}_4 \cdot 2\text{H}_2\text{O}$ at 25°C . Different compositions have been studied as shown in Table II which also gives the compositions of corresponding manganites $\text{Mn}_{3-x}\text{Ni}_x\text{O}_4$ with $x = 3y$ and $0.5 \leq x \leq 1$.

Thermal decomposition does not lead directly to the required spinel structure. In fact, beyond 420°C , i.e. after the end of the decomposition, X-ray diffraction analysis (XRD) reveals a mixture of phases constituted of cubic Mn_2O_3 and rhombohedral NiMnO_3 .

Because of the high reactivity of the oxides, a thermal treatment of several hours at 900°C allows a simultaneous crystallization of these oxides in a unique spinel phase according to the reaction



for all values $0.50 \leq x \leq 1$. Thus the thermal schedule to obtain a pure manganite powder from an oxalate precursor is as follows: increase the temperature at 120°C h^{-1} , soak for 4 h at 900°C and decrease the temperature at 600°C h^{-1} .

2.2. X-ray diffraction studies

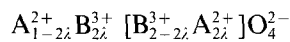
XRD powder patterns of the single-phase $\text{Ni}_x\text{Mn}_{3-x}\text{O}_4$ spinels were recorded at room temperature using an automatic diffractometer (Siemens D501 $\text{CoK}\alpha$ radiation). The standard error on parameter a was less than $\pm 0.0005 \text{ nm}$.

The general formula of oxide compounds which possess the spinel structure, based on the cubic

TABLE I Cation distributions of defined NiMn₂O₄ proposed in the literature

References	Year	Technique employed	Cation distributions
Sinha <i>et al.</i> [7]	1957	X-ray diffraction	Mn ²⁺ [Ni ²⁺ Mn ⁴⁺]O ₄ ²⁻
Azaroff [8]	1959	Neutron diffraction	Mn[NiMn]O ₄
Larson <i>et al.</i> [9]	1962	X-rays, thermoelectric data	Mn _{0.65} ²⁺ Mn _{0.35} ³⁺ [Ni ²⁺ Mn _{0.35} ³⁺ Mn _{0.65} ⁴⁺]O ₄ ²⁻
Boucher <i>et al.</i> [10]	1969	Neutron diffraction	Mn _v Ni _{1-v} [Ni _v Mn _{2-v}]O ₄ with 0.7 < v < 0.9
Bhandage and Keer [11]	1976	Thermoelectric data	Mn ³⁺ [Ni ²⁺ Mn _{0.10} ²⁺ Mn _{0.90} ³⁺]O _{3.95} ²⁻
Meenakshisundaram <i>et al.</i> [12]	1982	X-ray diffraction	Ni _{0.12} ²⁺ Mn _{0.88} ³⁺ [Ni _{0.88} ²⁺ Mn _{0.12} ³⁺]O ₄ ²⁻
Brabers and Terhell [13]	1982	Electrical conductivity	Ni _{1-y} ²⁺ Mn _y ²⁺ [Ni _y ²⁺ Mn _{2-2y} ³⁺ Mn _y ⁴⁺]O ₄ ²⁻ value of y is not given
Macklen [14]	1986	Electrical conductivity at 900°C	Ni _{0.35} ²⁺ Mn _{0.65} ²⁺ [Ni _{0.65} ²⁺ Mn _{0.70} ³⁺ Mn _{0.65} ⁴⁺]O ₄ ²⁻
Golestani-Fard <i>et al.</i> [15]	1987	Thermodynamic considerations	Mn _{0.83} ²⁺ Ni _{0.17} ²⁺ [Mn _{1.66} ³⁺ Ni _{0.49} ²⁺]O ₄ ²⁻
Islam and Catlow [16]	1988	Energetic electronic processes	Ni _{1-v} ²⁺ Mn _v ³⁺ [Ni _v ²⁺ Mn _{2-v} ³⁺]O ₄ ²⁻ v ≈ 0.9

close-packing of oxygen ions in which the cations are located on both tetrahedral and octahedral sites is



where λ is the degree of inversion, $0 \leq \lambda \leq 0.5$; the brackets indicate octahedral sites.

The cubic spinel structure is preserved when different kinds of cation occupy a spinel site. From this Poix [17, 18] points out the invariant character of the ‘‘anion–cation’’ distance for a particular site. Thus two parameters are defined, $d_A = A-O$ and $d_B = B-O$, where d_A and d_B are the mean values of the ‘‘anion–cation’’ distance in tetrahedral and octahedral sites, respectively. The lattice parameter a (nm) is related to d_A and d_B according to

$$a = 2.0995 d_A + (5.8182 d_B^2 - 1.4107 d_A^2)^{1/2}$$

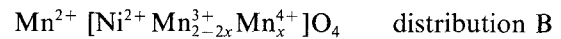
It may be seen that the theoretical lattice parameters could be calculated for various cation distributions among the two sublattices. From lattice energy considerations the presence of Ni³⁺ in nickel manganite is unlikely. In good agreement with previously published data [14], four cations Mn⁴⁺, Mn³⁺, Mn²⁺ and Ni²⁺ will be considered in the following discussion. The cation–oxygen distances used are given in Table III.

3. Results and discussion

All solid solutions Ni_xMn_{3-x}O₄ with $0.5 \leq x \leq 1$ crystallize with cubic symmetry (Table II). Fig. 1 (curve Ex) displays the evolution of a for Ni_xMn_{3-x}O₄ solid solutions as a function of the nickel content, x . Villers and Buhl [19] have shown that a of the defined compound NiMn₂O₄ varies with quenching temperature. In the present study, $a = 0.839$ nm for a quenching temperature of 900°C is in good agreement with previous results, corresponding to the same quenching temperature range [7, 9, 11].

It is now commonly accepted that the cation distribution in haussmannite Mn₃O₄ (the basic crystal

structure of manganites) is Mn²⁺ [Mn₂³⁺]O₄ [8, 20–22]. Thus the nickel cation can occupy either the tetrahedral site (A sites, Mn²⁺ substitution) or the octahedral sites (B sites, Mn³⁺ substitution). In the latter case, to preserve the overall electrical neutrality of the material, some of the Mn³⁺ on the B sites will change its valency to Mn⁴⁺. Thus two limiting ionic configurations can be proposed



Haussmannite exhibits a tetragonal distortion from cubic symmetry, explained by the presence of Mn³⁺ ions in octahedral positions (Jahn–Teller effect). Baffier and Huber [23] have pointed out that the existence of the tetragonal distortion in ferromanganite spinels depends on the concentration of Mn³⁺ ions. They should be in about 50% of the octahedral sites to give rise to a tetragonal distortion. For a Mn³⁺ concentration below this value, no tetragonal distortion appeared. Moreover, according to Dunitz and Orgel [24], if Ni²⁺ is located in tetrahedral sites, a tetragonal distortion with $c/a > 1$ is expected.

Remember that Ni_xMn_{3-x}O₄ with $0.5 \leq x \leq 1$ solid solutions crystallize in the cubic system; therefore, we can infer, on the one hand, that the Mn³⁺ ion concentration in octahedral sites is lower than 50% and, on the other hand, that Ni²⁺ cannot be situated in tetrahedral sites. For these reasons the cation distribution A can be eliminated.

In Fig. 1, the variation of the lattice parameter of Ni_xMn_{3-x}O₄ as a function of the nickel content, x ($0.5 \leq x \leq 1$), calculated for the cation distributions A and B, is compared with the experimental data. This comparison also allows us to rule out unambiguously the limiting distribution A; however, the experimental data do not fit the B distribution line snugly; a small amount of Ni²⁺ must be present in A sites.

 TABLE II Composition of oxalic precursors Mn_{1-y}Ni_y(C₂O₄) · 2H₂O and corresponding manganites Mn_{3-x}Ni_xO₄ which have been prepared in this work. The lattice parameter a of Mn_{3-x}Ni_xO₄ is given

y	0.20	0.22	0.23	0.25	0.26	0.27	0.28	0.32	0.33
x	0.60	0.65	0.70	0.75	0.77	0.80	0.84	0.95	0.99
a (nm)	0.845 ₄	0.844 ₁	0.843 ₈	0.843 ₀	0.843 ₀	0.842 ₅	0.841 ₈	0.840 ₂	0.839 ₈

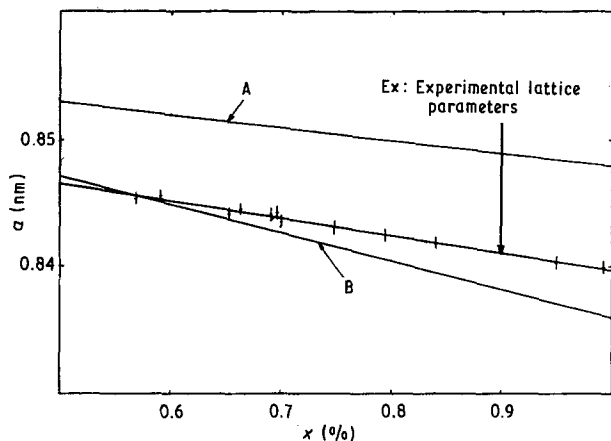
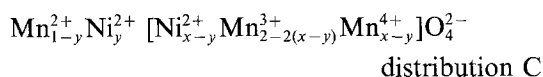


Figure 1 Variation of the lattice parameter of $\text{Ni}_x\text{Mn}_{3-x}\text{O}_4$ as a function of nickel content, x . Ex, experimental data; A and B lines, calculated for the cation distributions A $\text{Mn}^{2+}\text{Ni}^{2+}[\text{Mn}^{3+}]\text{O}_4^{2-}$, and B $\text{Mn}^{2+}[\text{Ni}_x^{2+}\text{Mn}_{2-x}^{3+}\text{Mn}_x^{4+}]\text{O}_4^{2-}$, respectively.

The theoretical variation of the lattice parameter a has been calculated (Poix method) for cationic distributions with 10%, 15%, 20%, 25%, 30% and 35% nickel content in tetrahedral A sites. The results are plotted in Fig. 2 together with experimental data. Because the experimental line cuts all the other lines, it can be inferred that the amount of nickel in tetrahedral sites increases with the overall nickel content x . Let P be percentage of Ni^{2+} in A-sites and x the number of nickel ions in the solid solutions the relationship $P = f(x)$ can be calculated (Fig. 3)

$$P = -82.1x^2 + 192.4x - 81.5 \quad (1)$$

Thus the general formula for the solid solutions is



with

$$y = xP/100 \quad (2)$$

We recall that, to a first approximation, the semi-conducting properties of manganites are described by a hopping mechanism (electron transfer) between Mn^{4+} and Mn^{3+} . The maximum conductivity of the material will be determined by the maximum number of ions involved in this electron transfer. Thus the

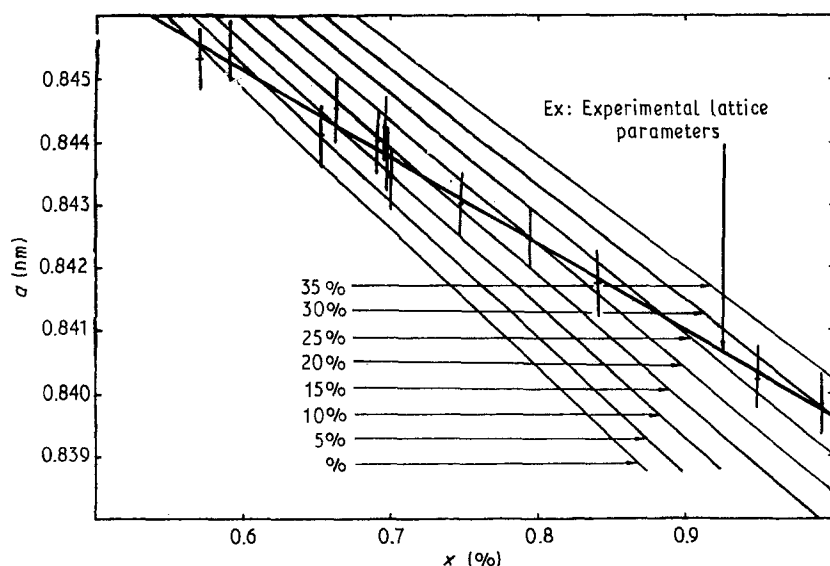


Figure 2 The theoretical variation of the lattice parameter a calculated (Poix method) for cationic distributions with 10%, 15%, 20%, 25%, 30% and 35% nickel content in tetrahedral A sites.

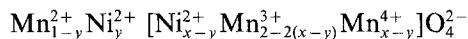
TABLE III The "anion-cation" distance (nm) in tetrahedral and octahedral sites of cubic spinel structure according to Poix [17, 18]

	Octahedral	Tetrahedral
$\text{Mn}^{4+}-\text{O}$	0.1843	—
$\text{Mn}^{3+}-\text{O}$	0.2045	—
$\text{Mn}^{2+}-\text{O}$	—	0.2041
$\text{Ni}^{2+}-\text{O}$	—	0.1970

shape of the resistivity curves as a function of the nickel content (x) will be different according to the sites of nickel ions in the spinel lattice. The resistivity will reach a minimum when the number of charge carriers reaches a maximum, i.e. when the number of Mn^{3+} ions is equal to the number of Mn^{4+} ions.

Taking into account the variation of the number of $\text{Mn}^{3+}-\text{Mn}^{4+}$, the theoretical variations of resistivity can be plotted against the nickel content for various distributions. In Fig. 4, the variations of experimental and theoretical resistivities with various nickel contents are presented.

In cation distribution A, Mn^{3+} ions only are present in octahedral sites, the structures do not allow electrical conductivity (Curve i). Curve (ii) shows the theoretical variation for cation distribution B (all Ni^{2+} in a B-sites) with a minimum of resistivity for $[\text{Mn}^{3+}] = [\text{Mn}^{4+}]$, i.e. $2 - 2x = x$ or $x = 0.66$. Curve (iii) corresponds to the cation distribution C proposed in this paper



with the calculation of the minimum of resistivity, i.e. $2 - 2(x - y) = x - y$ giving $x - y = 0.66$ setting y equal to $xP/100$ (Equation 2) and assuming Equation 1 for P we can calculate $x = 0.89$.

Finally, in a previous work, Jabry *et al.* [2] measured the resistivity of nickel manganite ceramics as a function of nickel content (x). The results obtained are shown in Fig. 4, Curve (iii) and a minimum of resistivity is found for $x = 0.80$. Once more the cation distribution A (Fig. 4, Curve i) can be ruled out because the material would be insulating in opposition with experimental data, Curve iv. Comparison of Curves

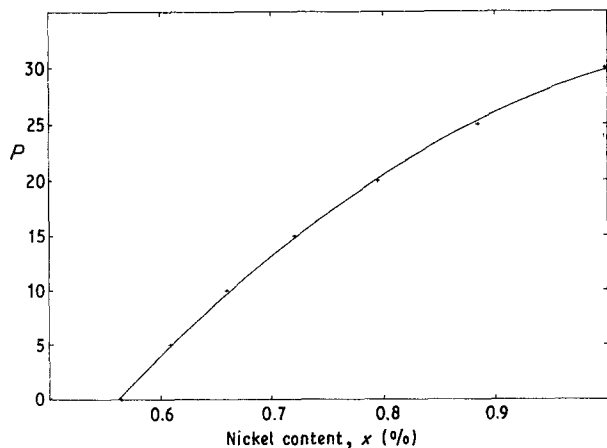
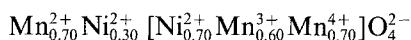


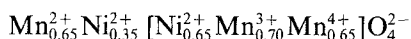
Figure 3 Percentage of nickel in A sites as a function of nickel content, x .

(ii) and (iii) clearly indicates that some Ni^{2+} are located in tetrahedral sites. Nevertheless, the experimental value (0.80) of the minimum of resistivity differs from the value (0.89) calculated from the cation distribution proposed in this work. This discrepancy in results can be explained by the fact that the hopping mechanism depends not only on the number of charge carriers but also on the distance between the charge carriers (the distance itself depends on the lattice parameter). Moreover, the screening effect of Ni^{2+} in octahedral sites can be taken into account. Note that in the cation distribution established in this paper the number of Ni^{2+} in octahedral sites increases with the overall nickel content.

For each sample of the solid solutions the percentage, P , of Ni^{2+} can be calculated, in A sites thus for the defined compound NiMn_2O_4 ($x = 1$) the $P = 28.8\%$ and the distribution of cations is



These results are in good agreement with the studies of electrical conductivity at high temperature obtained by Macklen [14] who concludes that the valence distribution of NiMn_2O_4 should be represented by



4. Conclusion

From mixed oxalic precursors, nickel manganites with cubic spinel structure $\text{Ni}_x\text{Mn}_{3-x}\text{O}_4$ ($0.5 \leq x \leq 1$) have been obtained with high purity at 900°C . The evolution of lattice parameter a of the solid solutions implies that the nickel ions occur in octahedral sites of the spinel structure. Therefore, for $x > 0.56$, some Ni^{2+} ions remain in tetrahedral sites. The percentage of nickel in A sites increases with nickel content, x , following the relationship

% Ni^{2+} in A sites = $P = -82.1x^2 + 192.4x - 81.5$
and thus the general formula for cation distribution is



with $y = xP/100$. This relationship explains the electrical properties of semiconducting nickel manganite ceramics.

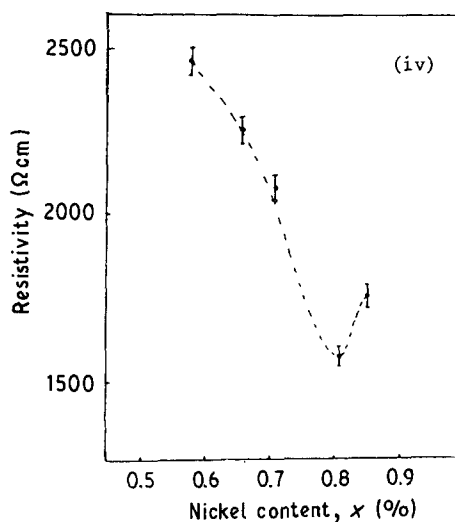
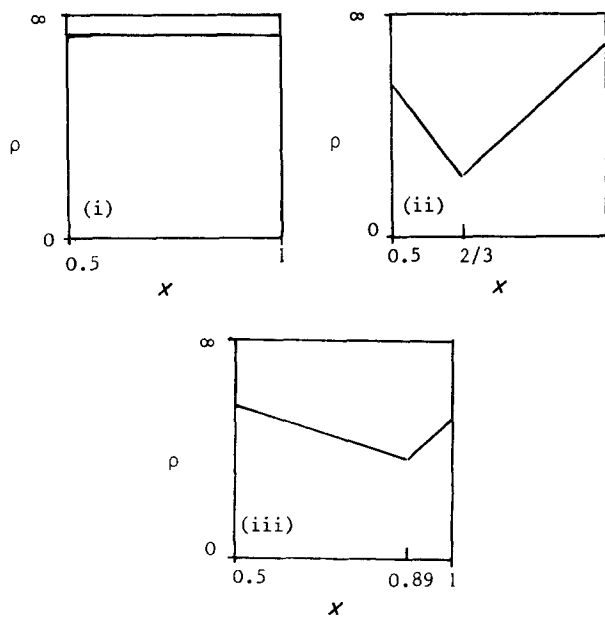


Figure 4 Theoretical variation of the electrical resistivity, only taking into account the variation in the number of $\text{Mn}^{3+}/\text{Mn}^{4+}$ ion pairs on octahedral sites as a function of nickel content, x , for a various distributions. (i) A, $\text{Mn}_{1-x}^{2+}\text{Ni}_x^{2+}[\text{Mn}_x^{3+}]\text{O}_4^{2-}$. (ii) B, $\text{Mn}^{2+}[\text{Ni}_x^{2+}\text{Mn}_{2-2x}^{3+}\text{Mn}_x^{4+}]\text{O}_4^{2-}$. (iii) Established in this work, $\text{Mn}_{1-y}^{2+}\text{Ni}_y^{2+}[\text{Ni}_{x-y}^{2+}\text{Mn}_{2-2(x-y)}^{3+}\text{Mn}_{x-y}^{4+}]\text{O}_4^{2-}$. (iv) Change of resistivity with the nickel content, experimental data [2].

References

1. E. D. MACKLEN, "Thermistors" (Electrochemical Publications, Ayr, Scotland, 1979).
2. E. JABRY, G. BOISSIER, A. ROUSSET, R. CARNET and A. LAGRANGE, *J. Physique* **46** (1986) C1 843.
3. J. P. CAFFIN, A. ROUSSET, R. CARNET and A. LAGRANGE, in "High-Tech Ceramics", edited by P. Vincenzini (Elsevier, Amsterdam, 1987) p. 1743.
4. R. LEGROS, R. METZ, J. P. CAFFIN, A. LAGRANGE and A. ROUSSET, in "Better Ceramics Through Chemistry III", edited by C. J. Brinker *et al.* (Elsevier, New York, 1988) **121**, p. 251.
5. R. METZ, J. P. CAFFIN, R. LEGROS and A. ROUSSET, *J. Mater. Sci.* **24** (1989) 83.
6. E. J. W. VERWEY, P. B. BRAUN, E. W. GORTER, E. C. ROMEIJN and J. H. VAN SANTEN, *Z. Phys. Chem.* **198** (1951) 6.
7. P. B. SINHA, N. R. SANJANA and A. B. BIWAS, *Acta Crystallogr.* **10** (1957) 439.
8. L. V. AZAROFF, *Z. Kristal.* **112** (1959) S33.
9. E. G. LARSON, R. J. ARNOTT and D. G. WICKHAM, *J. Phys. Chem. Solids* **23** (1962) 1771.

10. B. BOUCHER, R. BUHL and M. PERRIN, *Acta Crystallogr.* **B25** (1969) 2326.
11. G. T. BHANDAGE and H. V. KEER, *J. Phys. C Solid State Phys.* **9** (1976) 1325.
12. A. MEENAKSHISUNDARAM, N. GUNASEKARAN and V. SRINIVASAN, *Phys. Status Solidi (a)* **69** (1982) K15.
13. V. A. M. BRABERS and J. C. J. M. TERHELL, *ibid.* **69** (1982) 325.
14. E. D. MACKLEN, *J. Phys. Chem. Solids* **47** (1986) 1073.
15. F. GOLESTANI-FARD, S. AZIMI and K. J. D. MACKENZIE, *J. Mater. Sci.* **22** (1987) 2847.
16. M. S. ISLAM and C. R. A. CATLOW, *J. Phys. Chem. Solids* **49** (1988) 119.
17. P. POIX, *Bull. Soc. Chim. France* **5** (1965) 1085.
18. *Idem*, *C.R. Acad. Sci. Paris* **268** (1969) 1139.
19. G. VILLERS and R. BUHL, *ibid.* **260** (1965) 3406.
20. J. B. GOODENOUGH and A. L. LOEB, *Phys. Rev.* **98** (1955) 391.
21. P. K. BALTZER and J. G. WHITE, *J. Appl. Phys.* **29** (1958) 445.
22. R. BUHL, *J. Phys. Chem. Solids* **30** (1969) 805.
23. N. BAFFIER and M. HUBER, *ibid.* **33** (1972) 737.
24. J. D. DUNITZ and L. E. ORGEL, *ibid.* **3** (1957) 20.

*Received 4 May
and accepted 29 September 1989*